

## ACOUSTICAL PARAMETERS OF SODIUM BORATE METALLIC GLASS - $\text{Na}_2\text{CO}_3\text{-B}_2\text{O}_3\text{-Na}_2\text{O}$

D. PRIYA<sup>a,\*</sup>, S. THIRUMARAN<sup>b</sup>

<sup>a\*</sup> *Research Scholar, Department of Physics, Manonmaniam Sundaranar University, Tirunelveli, India*

<sup>b</sup> *Professor, Department of Physics, Annamalai University, Chidambaram, India*

In recent decades, one of the very popular and kind of advanced materials is Metallic glasses. Metallic glass materials can easily versatile for their manufacturability with plastics because of their complex shapes. Presently, Glassy alloys pivot an extraordinary exploration in the worldwide community of metals. In this paper we have presented about Sodium Borate Glass-( $\text{Na}_3\text{BO}_3$ ) nature, glasses in the system  $\text{Na}_3\text{BO}_3$ , by melt quenching technique has been prepared. The structural investigation has been carried out by X-Ray Diffraction studies. Debye temperature and Elastic properties have been analyzed by utilizing measurements of sound velocity. The purpose of  $\text{Na}_2\text{O}$  in the  $\text{B}_2\text{O}_3$  is to change the host structure by changing the borate network structural units from  $\text{BO}_3$  to  $\text{BO}_4$ . Sodium diborate is a type of borate glass. Borate glass of this type attracts many researchers attention because of their improved optical and electrical properties. Infra Red spectroscopy is one of the viable tools for the local arrangements structure resolution in glasses. The UV visible optical analysis is used to study about the optical spectra. These results are utilized to find the refractive index of glasses and optical band gap.

(Received December 30, 2020; Accepted March 12, 2021)

*Keywords:* Metallic glasses, Elastic property, Debye temperature, SEM analysis, Sodium borate glass

### 1. Introduction

From the past few decades there was a thought saying it's impossible to form stable glasses for pure metals. Current research supports formation of glass in pure metals past evidences, represents the devices potential based on quick crystal-glass phase change, and also features the adequate theory lacking for fast growth of crystals. Metallic glasses are an interesting metallic materials class which does not show long-range atomic order. Because of their concomitant lack of dislocations and amorphous character these materials shows mechanical properties that are very not the same as those of other solid materials [1]. For instance, it can be twice as solid as steels, show better fracture toughness and elasticity as ceramics and less weak than conventional oxide glasses. Notwithstanding their mechanical properties uniqueness, metallic glasses likewise exhibited fascinating chemical and physical properties [2]. Few metallic glasses have found to exhibit predominant properties of soft magnets, outstanding catalytic performance and good magneto caloric effects, along these having potential for a far and wide scope of applications in technology.

Glasses of Alkali oxy borate are notable because of their assortment of phosphors utilization, in number of electronic devices and solar energy converter. A metallic glass has high mechanical strength when contrasted with the pure borate glasses. The acoustical properties are especially reasonable for portraying glasses as a composite capacity since they provide little information about both the dynamics of glasses and the microstructure. The elastic properties are identified with microscopic properties through the modifier and network behavior. Various tests were carried to interpret and measure the borate glass acoustical properties as far of structural changes. From the tests found that the addition of  $\text{Na}_2\text{O}$  to vitreous  $\text{B}_2\text{O}_3$  increases the ultrasonic velocity because of the variations in boron atom co-ordination number from 3 to 4. For high

---

\* Corresponding author: priyalecturer@rediffmail.com

technological applications Borate glasses are highly suitable. The boron atom in glasses and borate crystals typically coordinate with one or the other 3 or 4 oxygen forming structural units ( $\text{BO}_3$ ) or ( $\text{BO}_4$ ). The alkali tetra borate glasses are generally utilized materials in the opto-acoustical electronics field in non-linear devices for the conversion of frequency in the piezoelectric actuator and ultraviolet region. Then, their crystalline counterparts and these glasses are acceptable possibility for the optically prompted elasto-opticity. In sodium borate glasses generally structural groupings are of three types found to be specific tetra borate units, diborate and boroxol rings units. All these groups show boron configurations of two distinct kinds. In the groups of high sodium borate glasses tetra borate are revamped one  $\text{Na}_2\text{O}$  and rearranged two diborate units to the detrimental tetra borate unit with  $\text{BO}_4$ .

Therefore one  $\text{Na}_2\text{O}$  structure the two  $\text{BO}_4$  units to form the three dimensional structure networks. To know about the solids structure and they are straight forwardly identified with interatomic potentials elastic properties are very informative. Currently researchers have showing more interest on glassy materials due to their high optical quality and larger optical nonlinearity with quick time of response. Ultrasonic apparatus are significant in materials portraying since they have numerous applications in chemistry, physics, medicine, food industry, oceanography etc. One of the outstanding amongst other glass formers is Boron oxide and its structure comprises an arrangement of sheet like boron-oxygen triangles associated with all corners to frame a network continuously. Borate glasses physical properties can regularly be changed by the expansion of a normally utilized network modifier to the essential constituent.

The acoustical properties are incompletely reasonable for depicting glasses as a composition function since they give some data about the dynamics of the glasses and the micro structure. The ultrasonic Non Destructive Testing (NDT) has discovered to be perhaps the better methods to the microstructure examination, mechanical properties characterization and the phase changes just as to assess elastic constants. In this paper,  $\text{B}_2\text{O}_3 - \text{Na}_2\text{CO}_3 - \text{Na}_2\text{O}$  (BSS glass system) is discussed.

The ultrasonic velocity and density for the glass systems have been measured by pulse echo technique by Archimedes' principle. The elastic constants like Shear modulus (S), longitudinal modulus (L), Young's modulus (E), bulk modulus (K), acoustic impedances (Z), Poisson's ratio ( $\sigma$ ), Debye temperature ( $\theta_D$ ), micro hardness (H) and co-efficient of thermal expansion ( $\alpha_p$ ) has measured which gives more important information about the structure of borate glass and rigidity. The XRD, spectroscopic, scanning electron microscopic (SEM) and UV studies to substantiate their structural elucidation analysis are also been carried out for the glass.

## 2. Experimental details

The current research work AR, SR grade chemicals were used with 99% least measure were gotten. Table 1 shows the  $\text{B}_2\text{O}_3$  mol% composition is kept steady and fluctuating the  $\text{Na}_2\text{O}$  mol% in BSS-glass system and glass substance. The necessary quantity (roughly twenty grams) of chemicals in mol% was gauged by utilizing a digital balance solitary pan having 0.0001 g accuracy. The appropriate mixture homogenization of the chemicals component was affected by consistently granulated.

The blend is heated with the help of platinum crucible and temperature is controlled through a muffle furnace after few hours at certain point it was raised step by step to at the rate of 100k/hour in higher temperature, BSS glass system glassily structure is formed at 1400 K. In the heavy copper molding block having the dimension of 5 mm diameter and 10 mm length, molten glass melt was quickly poured and without any disturbance kept at room temperature. Then the glass sample was annealed at 400 K for two hours to avoid the mechanical strains developed during the quenching process. The two opposite faces of glass were highly polished to ensure a good parallelism. All glasses are cleaned with acetone to remove the presence of any foreign particles. The samples are prepared by chemically stable and non-hygroscopic and such glass samples System (BSS) are reported in Plate for analysis.

Table 1.  $B_2O_3$  mol% composition

CONCENTRATION	$B_2O_3$ %	$Na_2CO_3$ %	$Na_2O$ %
S1C1	60	32	08
S2C2	60	29	11
S1C3	60	26	14
S1C4	60	23	17
S1C5	60	20	20

## 2.1. Characterization techniques

By using the pulse-echo method at room temperature at a frequency of 5 MHz with X-cut and Y-cut transducers were used to determine the glass specimen of the shear and ultrasonic longitudinal velocity. Transmitters and receivers both of these transducers go about as the two of the ultrasonic pulse. The transducer was bringing into contact with all the 12 samples by couplet method, to confirm that there was no air void in centre of the specimen and the transducer. On the probe constant pressure is applying continuously, the waveforms of echo were acquired store the memory on the display unit. The glass sample density was estimated utilizing the method of relative measurement. The glass sample weight was estimated in a single pan with 0.0001 g privacy. By utilizing the formula:  $\rho = \rho_B \frac{W_1 - W_2}{W_1}$ , where  $W_1$  and  $W_2$  are the glass samples weights in benzene and in air and  $\rho_B$  is the benzene density at 303 K density can be calculated. A PW1700 X-ray diffractometer was used with CuK as a radiation source somewhere in the range of  $20^\circ$  and  $80^\circ$ , of the prepared borate glass to find the nature.

## 3. Results

### 3.1. XRD analysis

XRD studies were carried out for the prepared glass to confirm the amorphous nature on the glass sample. The glass sample prepared with the help of double distilled water was washed gently. The glass sample washed were dried, ground, at room temperature and later utilized to get the XRD patterns. From the obtained spectrum we can clearly see the unmelted crystalline particles which confirm the amorphous nature, and also BSS glass system structure which is shown in Fig. 1 and the peak values are plotted.

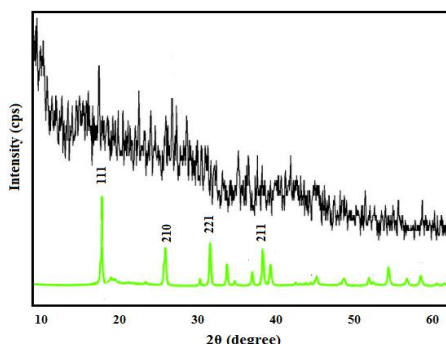


Fig. 1. BSS glass system structure.

### 3.2. FTIR analysis

FTIR spectra of BSS glass having between the wavelength regions  $400 - 4000 \text{ cm}^{-1}$  is shown in Fig. 2.

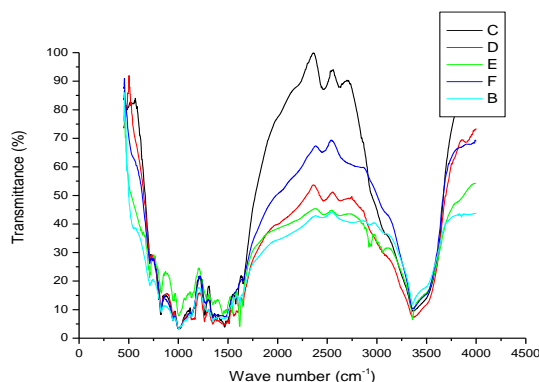


Fig. 2. FTIR spectra of BSS glass system.

The borate glass network vibration mode shows the presence of 3 regions of band in BSS glass system, bands which occur at  $1200 - 1600 \text{ cm}^{-1}$  is of the first group which is due to the B-O bonds in  $\text{BO}_3$  units symmetric stretching vibration, the 2<sup>nd</sup> group which is between  $800$  and  $1200 \text{ cm}^{-1}$  and is due to the tetrahedral  $\text{BO}_4$  units B-O stretching bond and last 3<sup>rd</sup> group is found at  $700 \text{ cm}^{-1}$  which is mainly because of B-O-B linkage in the borate network bending. The band of approximately  $1004 - 1007 \text{ cm}^{-1}$ ,  $1130$  and  $1022-1058 \text{ cm}^{-1}$  in BSS system is attributed to the asymmetric tetrahedral stretching vibrations of  $\text{BO}_4$  borate groups. The characteristic absorption bands around  $1577, 1558, 1578$  &  $1560 \text{ cm}^{-1}$  is assigned to the C-O ( $\text{Na}_2\text{CO}_3$ ) B-O stretching vibration in the BSS system. The bands at  $821, 826, 828 \text{ cm}^{-1}$  presence confirms specific bending vibrations of O-C-O linkage ( $\text{Na}_2\text{CO}_3$ ) and B-O,  $\text{BO}_4$  stretching vibration. The  $710 \text{ cm}^{-1}$  peak is assigned to the two trigonal oxygen atoms oxygen bridging vibration. This peak sharpness increases with respect to decreasing modifier content ( $\text{Na}_2\text{O}$ ), the high intensity of the bond around  $1300 \text{ cm}^{-1}$  for the content of increased modifier which indicates the NBOs presence because of pyroborate and metaborate chains. Similarly, it is understandable that the  $\text{Na}_2\text{CO}_3$  content increase will be accompanied by an increase in the ionic bonding degree in the system increases the anharmonic region. Those bands intensity changes which is inter related with this glass system properties change.

Table 2. Shows the strong dependence of the network modification.

BAND POSITION					ASSIGNMENTS
S1C1	S1C2	S1C3	S1C4	S1C5	
3364	3376	3358,3059	3362	3361	Antisymmetric & symmetric stretching vibration of H <sub>2</sub> O molecules
2634	2633	2921			
2458	2460				
1654	1652	1648	-	1618	Bending vibration of H <sub>2</sub> O molecule, change from $\text{BO}_3$ to $\text{BO}_4$
1577	1558	1578,1542			B-O stretch in $\text{BO}_3$ units
1467	1461	1448			B-O stretching vibrations of trigonal units
1390	1396	1392	1346	1347	Antisymmetric stretching vibration of B-O trigonal units
1267	1263	1292	1279		B-O stretching vibrations
1130	1131	1129	1130		B-O stretching vibrations
1004	1006	1005	1007	1005	Pentaborate groups.
946	943	956	945		B-O linkages Stretching vibrations in tetrahedral units
821	827	828	826	828	tri, tetra and penta borate groups Stretching vibrations
	710	710	712	711	$\text{BO}_3$ & $\text{BO}_4$ groups Bending vibrations
475				465	Cation vibrations

$\text{Na}_2\text{O}$  acts as a modifier generally;  $\text{Na}^+$  ions occupy the interstitial positions while these oxides of oxygen breaks the local symmetry and co-ordinate defects introducing in the system said to be dangling bonds with non-bridging oxygen's. The band intensity at  $1267\text{cm}^{-1}$  decreases with increasing  $\text{Na}_2\text{CO}_3$  content. From the results obtained and from the FTIR studies it confirms various content of Borate network (ie.,  $\text{BO}_3$  &  $\text{BO}_4$ ) presence in the glass system. The results presented here, together with available literature point tabulated in Table (2) shows the strong dependence of the network modification on the nature of the cationic modifier (Na). The  $\text{Na}^+$  ion seems to be favoring the distribution of borate network.

### 3.3. Infrared absorption spectra (IR):

The sample of IR absorption spectra shows the IR bands which are triangular and tetrahedral borate units together the characteristics with some little bands because of OH and B-OH. The obtained glass system of IR spectra is mainly shows the modified borate networks and active in  $400\text{-}600\text{ cm}^{-1}$  spectral range. This large spectrum's is shown in the range of  $450\text{-}2000\text{ cm}^{-1}$  for clear understanding.

Fig.2 shows the borate glasses IR results which represents the four distinct regions. From  $1200\text{-}1600\text{ cm}^{-1}$  and from  $800\text{-}1200\text{ cm}^{-1}$  these two regions are referring to the both triangular  $\text{BO}_3$  and tetrahedral  $\text{BO}_4$  borate units stretching vibrations respectively. Both types units deformation mode near  $600\text{-}800\text{ cm}^{-1}$  are very active. The band between  $825$  and  $1130\text{ cm}^{-1}$  are attributed to the tetrahedral  $\text{BO}_4$  B-O stretching vibrations. The band at around  $1258\text{ cm}^{-1}$  is due to the B-O bonds stretching vibrations of  $\text{BO}_3$ - which involves the different group linkage oxygen connection. The peaks appeared at  $1560\text{-}1580\text{ cm}^{-1}$  is assigned as  $\text{BO}_3$  unit's anti-symmetrical stretching vibration. The peak at  $1650\text{ cm}^{-1}$  represented that  $\text{BO}_3$  changes to  $\text{BO}_4$  and also the peak may due to molecular water bending vibrational mode.

Table 3. Ultrasonic velocity, Elastic moduli and density values with respect to mol%  $\text{Na}_2\text{O}$  change.

Name of the sample	Density $\rho$ ( $\times 10^3\text{ kg. m}^{-3}$ )	Ultrasonic Velocity $U$ ( $\text{m.s}^{-1}$ )		Elastic moduli			
		Longitudinal ( $U_1$ )	Shear ( $U_s$ )	Longitudinal $L$ ( $\times 10^9\text{ N.m}^{-2}$ )	Shear $G$ ( $\times 10^9\text{ N.m}^{-2}$ )	Bulk $K$ ( $\times 10^9\text{ N.m}^{-2}$ )	Young's $E$ ( $\times 10^9\text{ N.m}^{-2}$ )
S1C1	2450.9	3987.09	2190.5	39.0	11.8	23.3	30.2
S1C2	2442	3980.93	2187.12	38.7	11.7	23.1	30.0
S1C3	2432.6	3970.58	2181.43	38.4	11.6	22.9	29.7
S1C4	2423.5	3959.38	2175.28	38.0	11.5	22.7	29.4
S1C5	2416.6	3947.09	2168.72	37.6	11.4	22.5	29.2

Most of the inorganic materials occur in hygroscopic form so; the peaks established at  $3360\text{-}2636\text{ cm}^{-1}$  are shows symmetric stretching vibration and antisymmetric of water molecules found in the glasses. The different glass specimens ultrasonic velocity [both longitudinal and shear] and density values with respect to mol%  $\text{Na}_2\text{O}$  change is shown in Table 2. The elastic moduli such as longitudinal modulus (L), shear modulus (G), bulk modulus (K), and young's modulus (E) are tabulated in Table 3. Table 4 shows the Poisson's ratio ( $\sigma$ ), acoustic impedance (Z), micro hardness (H), Debye temperature ( $\theta_D$ ) and thermal expansion co-efficient ( $\alpha_p$ ) values for the glass systems BSS. Figure 3 shows the variation of Debye temperature of  $\text{Na}_2\text{O}$  (mol), bulk modulus, shear modulus, acoustical impedance, microhardness, poissons ratio.

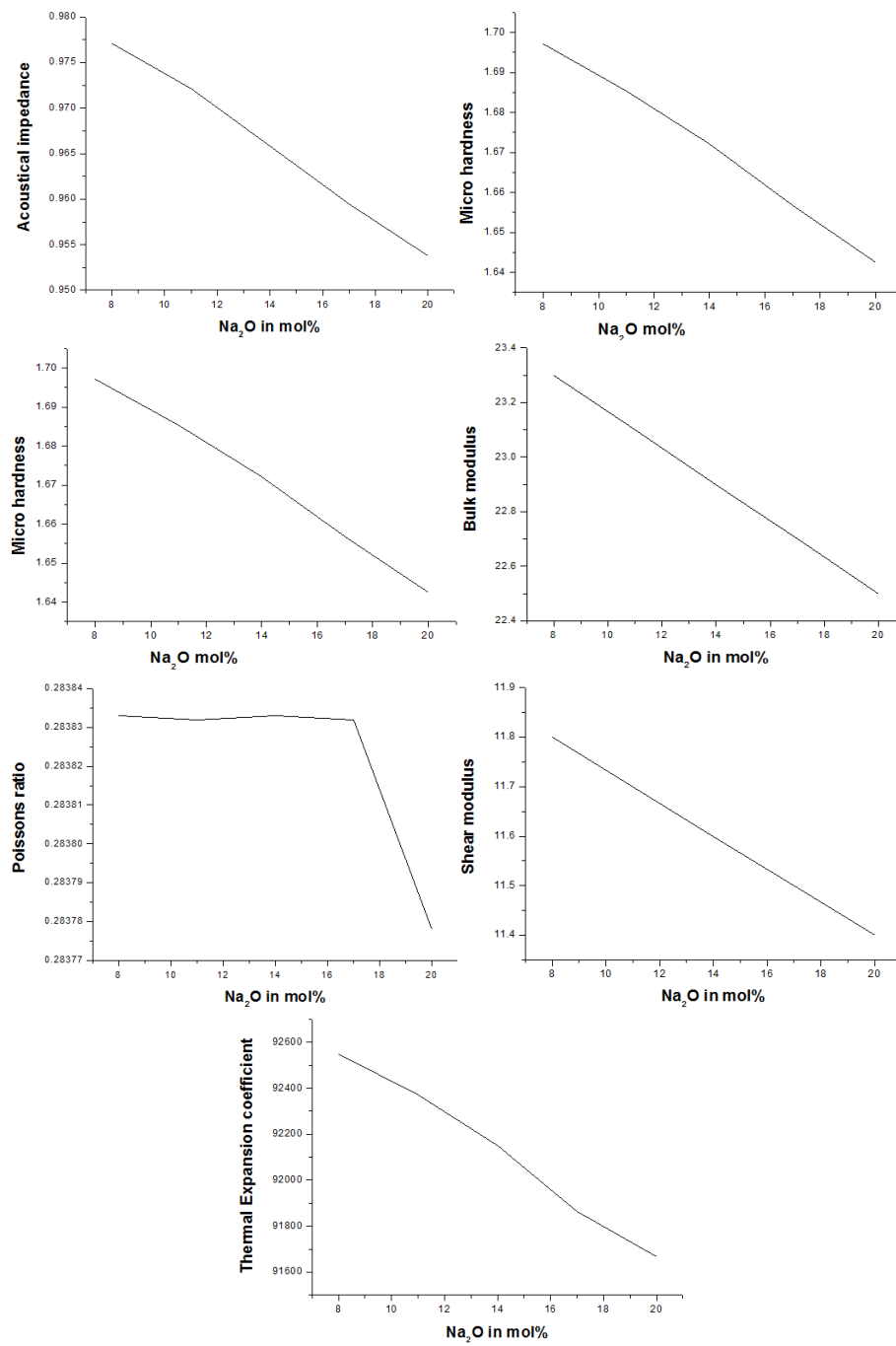


Fig. 3. Shows the variation of Debye temperature of Na<sub>2</sub>O (mol), bulk modulus, shear modulus, acoustical impedance, microhardness, poissons ratio.

Table 4. Shows the micro hardness ( $H$ ), acoustic impedance ( $Z$ ), Debye temperature ( $\theta_D$ ), Poisson's ratio ( $\sigma$ ), and thermal expansion co-efficient ( $\alpha_p$ ) values for the glass systems BSS.

Name of the sample	Poisson's ratio ( $\sigma$ )	Acoustic impedance $Z/(\times 10^7 \text{ kg.m}^{-2} \text{ s})$	Micro hardness $H/(\times 10^9 \text{ N.m}^{-2})$	Debye temperature $\theta_D /(\text{K})$	Thermal expansion coefficient $\alpha_p /(\text{K}^{-1})$
S1C1	0.283833	0.9771	1.6972	281.56	92548.67
S1C2	0.283832	0.9721	1.6854	281.42	92370.43
S1C3	0.283833	0.9658	1.6723	283.34	92149.26
S1C4	0.283832	0.9595	1.6567	284.62	91865.83
S1C5	0.283778	0.9538	1.6425	286.24	91665.58

### 3.4. Density

In the field of science especially where the glass structure is concerned density plays an important physical property. The measurement of density is a sensitive tool which can easily find any structural change in the glass network. The  $\text{Na}_2\text{O}$  are modifiers network and present in  $\text{B}_2\text{O}_3$ - $\text{Na}_2\text{CO}_3$  glass interstitially and breakdown bridging bonds. The non-bridging oxygen's creation in the network is reduced decrease and connectivity density. Decreasing density values in the glass system of BSS may also be interpreted because of the  $\text{BO}_4$  unit formation due to inclusion of metal ion  $\text{Na}_2\text{O}$  contents. However, the inclusion of sodium ions  $\text{Na}_2\text{O}$  which positioned in the cavities of an empty band gap space of the network obstructing the formation of  $\text{BO}_4$  unit further and this makes the density to decrease. The decreases in density assure the less compact structure of the glass.

### 3.5. Ultrasonic behavior of BSS glass systems:

It is observed that both shear and longitudinal velocities of BSS systems mol% is lowering with increase of  $\text{Na}_2\text{O}$  respectively. The ultrasonic velocity decrease is connected with the number of non-bridging oxygen (NBO) increase and at the same time glass network connectivity decrease. It may also be interpreted as the decreasing velocities in BSS glass systems and it can be interpreted as due to the involvement of  $\text{Na}_2\text{O}$  ions as modifiers breaking up  $\text{B}_2\text{O}_3$  units and  $\text{O}_2$  of  $\text{Na}_2\text{O}$  ions tetrahedral bonds. Consequently, resulting in replacing of its symmetry of  $\text{B}_2\text{O}_3$  and its cations occupy the interstitial position. Rupturing the symmetry of tetrahedral  $\text{B}_2\text{O}_3$  network and a creation of negative charged atoms leads to the decrease in ultrasonic velocity, the inclusion of heavy metal leading the wave for decrease of ultrasonic velocities in the glassy matrix which results in ultrasonic wave's slower impedance to the propagation in the specimen.

### 3.6. Elastic behavior of BSS glass systems:

The elastic properties field information forces regarding that operate in the middle of ions or atoms in the solid materials. Kind of this information provides predominant clues in understanding and interpreting solid materials bonding nature. These properties help in explaining the glass structure as a function and its dimensionality, composition and the connectivity of glass structure. The elastic moduli decrease has been assigned to the non-bridging oxygen's presence and the glass network connectivity decrease.

### 3.6. Poisson's Ratio

In elastic analysis of materials Poisson's ratio play an significant material property. From the survey results observed where changes in cross-link density of the glass network Poisson's

ratio is affected and suggested that structure having large density cross link will have in the order of 0.1 to 0.2 Poisson's ratio while structures with low crosslink density in the order of 0.3 to 0.5 have Poisson's ratio. BSS glass system have Poisson's ratio 0.3 nearly and it shows that there glass structures possess low cross-link density.

### 3.7. Debye temperature

From the measured velocity Debye temperature ( $\theta_D$ ) can be directly obtained. It increases with  $\text{Na}_2\text{O}$  content mol% increase in BSS glass system. This Debye temperature raise may be because of the centre charge coming nearer than the required distance, while comparing with other data this shows a Columbian interaction more effectively. These kinds of interaction usually will result in increased energy vibrational modes, and at the same time it increases the Debye temperature.

### 3.8. Acoustical impedance

The acoustical impedance and the thermal expansion coefficient decrease with  $\text{Na}_2\text{O}$  mol% increase in BSS glass respectively. This confirms the rigidity decrease of the glass structure. Decrease in microhardness of glasses means softening point's reduction, increases as the network modifiers content.

### 3.9. UV-Vis Spectroscopy – Band gap determination using Tauc plot method

The UV-Vis spectrum is as shown in Fig. 4.

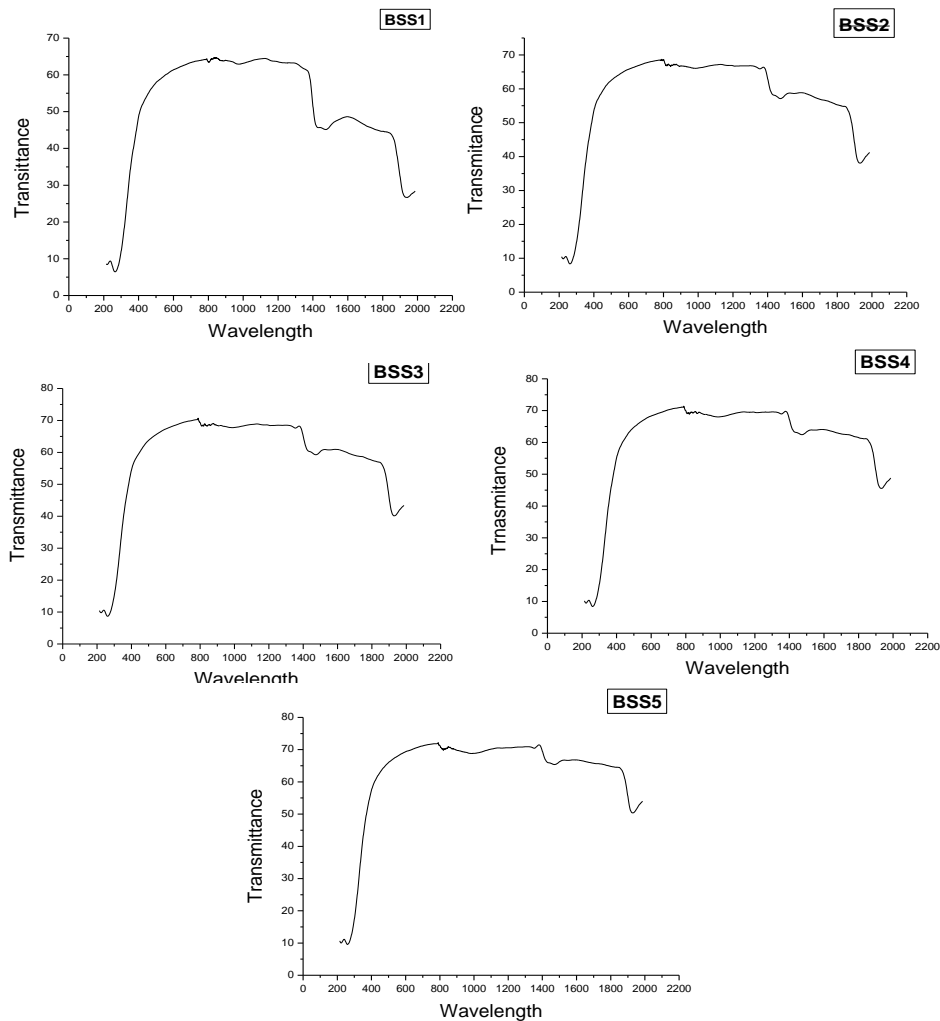


Fig. 4. UV-Vis spectrum.



Absorption co-efficient variation with photon energy in amorphous materials shows three regions. First region represents the ‘Tauc Region’ for high absorption. The 2<sup>nd</sup> region said to be ‘Urbach region’ is exponential region because of structural disorientations and randomness of the system. The 3<sup>rd</sup> region is the weak absorption tail produced from impurities and defects in the u-v spectra. The glasses fundamental optical band gap has been system based on its UV-Vis absorption spectra, for the clear view of the optically induced transition. Table [5] shows the various systems and its wavelength with respect to bandgap.

Table 5. Various bandgap values.

System	Wavelength maximum(nm)	Bandgap (eV)
S1C1	218	4
S1C2	280	4.41
S1C3	263	4.70
S1C4	247	5.50
S1C5	239	5.16

For photon energies  $h\nu$  just above the fundamental edge, the absorption  $\alpha$  follows the standards relation,  $\alpha = \frac{(h\nu - E_g)^{1/2}}{A}$ , where  $A$  is a constant and  $E_g$  is defined as the energy band gap. The value of  $E_g$  indirect transitions is obtained by extrapolation of  $(\alpha h\nu)^{1/2}$  versus  $h\nu$  plot to  $\alpha^{1/2} = 0$ . (2h3).

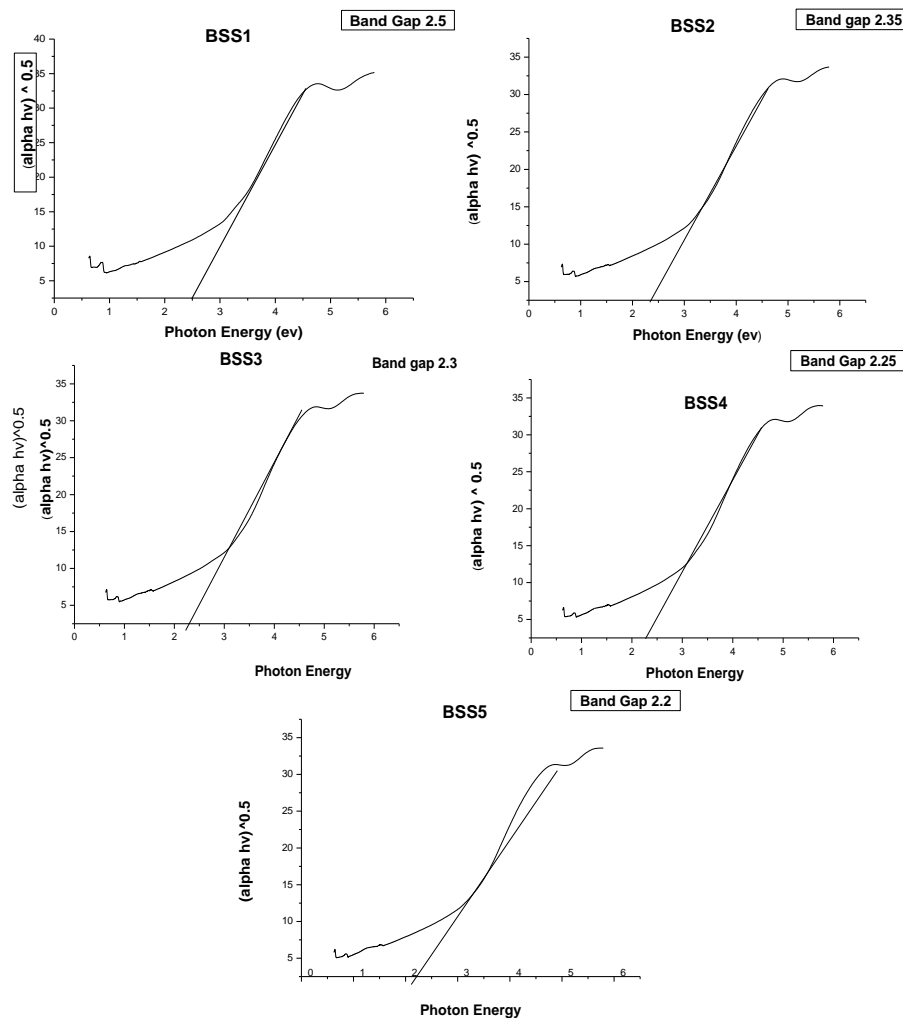


Fig. 5. Shows the plots for direct band gap of the sample.

Fig. 5 shows the plots for direct band gap and indirect band gap for the prepared samples and their values are tabulated in table [6]. In BSS glass system photon energy decreases with increasing  $\text{Na}_2\text{O}$  content. The addition of sodium ions increases localized electrons because of an increase in donor center in glass network, the presence of higher concentration of these donor centers decreases the optical band gap. In this glass system BSS  $\text{Na}_2\text{O}$  are glass modifiers. The addition of alkaline earth oxides and many other divalent metal oxides causes depolarization of the glass chain.

Table 6. Direct band gap and Indirect band gap for the prepared samples.

Mol%	Direct Bandgap	Indirect Bandgap
	$\text{Na}_2\text{O}$	$\text{Na}_2\text{O}$
08	3.68	2.50
11	3.65	2.35
14	3.60	2.30
17	3.55	2.25
20	3.51	2.20

Consequently, the average oxygen length is shortened. The addition of oxides also opened up the chain by breaking those bonds. In this way, the amount of NBO grows as the  $\text{Na}_2\text{O}$  concentrations in BSS glass systems increase, as described by the mechanism. This process changes the oxygen bonding in the glass-forming network, such as the formation of NBOs, will result in changes in the absorption characteristics. This alteration explains the decrease in the band gap with an increase in  $\text{Na}_2\text{O}$  contents.

Photon energy variation or different  $\text{Na}_2\text{O}$  mol% is shown in figure [5]. The photon energy value decreases linearly with  $\text{Na}_2\text{O}$  increasing contents in BSS glass system. This kind of variation is explained by the proposition that NBO content increases as the  $\text{Na}_2\text{O}$  contents increase shifting the band edge to higher energies and leading to photon energy value decrease. This photon energy value decrease confirms disorder in the glass network. Consequently there will be localized states with more extension within the band gap.

### 3.10. Scanning Electron Microscope (SEM)

To investigate the glass samples surface nature, scanning electron microscope analysis was carried out. SEM micrographs of BSS glass system are shown in the Fig. 6. It is seen that various measured grain particles are disseminated. The size of the particles appears to differ in each graph obtained. By nature these particles are very spherical and angular. These photographs represent clearly that there is no existing crystalline phase in the samples overall surfaces. The huge particles might be mono mineral; however is likely to be composite majority. Some sphere like agglomerates were seen spreading on the surface of glass because of the amorphous apatite deposition. This recommends that during the formation of glass, clusters presences formed by fibers are framed. Additionally, large particles may be present in the glasses, agglomerates, aggregates and bunches of clusters, which explains clearly the glass samples morphology surface.

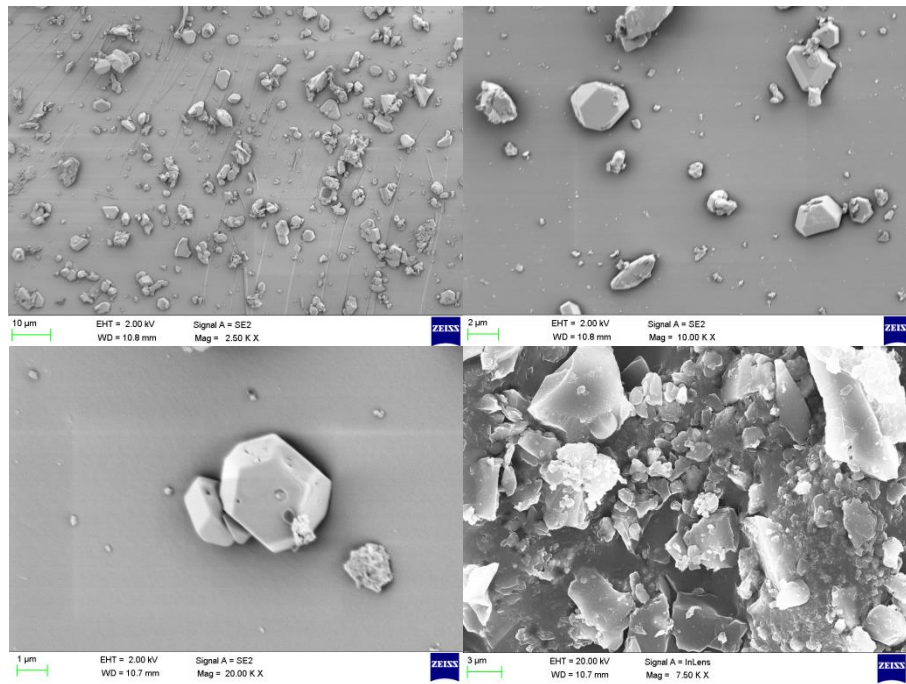


Fig. 6. SEM micrographs of BSS glass system.

#### 4. Conclusion

The band gap decrease with the  $\text{Na}_2\text{O}$  replacement content is credited to the  $\text{BO}_3$  triangular unit conversion into tetrahedral units of  $\text{BO}_4$  and NBOs increase. The band gap decrease confirms more tails extension of localized states into the band gap and subsequently structural changes in the glass network takes place with  $\text{Na}_2\text{O}$  replacement. It is very well concluded that the  $\text{Na}_2\text{O}$  glass network occupied in modifier position and hence plays as glass modifiers.

#### References

- [1] B. Svendsen, S. Bargmann, J. Mech. Phys. Solids **58**, 1253 (2010).
- [2] C. C. Hays, C. P. Kim, W. L. Johnson, Phys. Rev. Lett. **84**, 2901 (2000).
- [3] A. Dubach, R. Raghavan, J. F. Loffler, J. Michler, U. Ramamurty, Scr. Mater. **60**, 567 (2009).
- [4] M. I. Mendeleev, D. K. Rehbein, R. T. Ott, M. J. Kramer, D. J. Sordelet, J. Appl Phys. **102**, 093518 (2007).
- [5] H. S. Chen, Acta Metall. **22**, 1505 (1974).
- [6] A. Inoue, T. Nakamura, N. Nishiyama, T. Masumoto, Mater. Trans. **33**, 937 (1992).
- [7] B. Huang, H. Y. Bai, W. H. Wang, J. Appl. Phys. **110**, 123522 (2011).
- [8] W. H. Wang, C. Dong, C. H. Shek, Mater. Sci. Eng. R. **44**, 45 (2004).
- [9] K. F. Xie, K. F. Yao, T. Y. A. Huang, Intermetallics **18**, 1837 (2010).
- [10] N. C. Wu, L. Zuo, J. Q. Wang, E. Ma, Acta Mater. **108**, 143 (2016).
- [11] G. H. Zhang, K. C. Chou, J. Appl. Phys. **106**, 094902 (2009).
- [12] A. Takeuchi, A. Inoue, Mater. Trans. **46**, 2817 (2005).
- [13] O. N. Senkov, D. B. Miracle, Mater. Res. Bull. **36**, 2183 (2001).
- [14] D. C. Hofmann, J. Y. Suh, A. Wiest, M. L. Lind, M. D. Demetriou, W. L. Johnson, PNAS **105**, 20136 (2008).
- [15] J. W. Qiao, H. L. Jia, P. K. Liaw, Mater. Sci. Eng. R **100**, 1 (2016).
- [16] Y. Zhang, W. H. Wang, A. L. Greer, Nat. Mater. **5**, 857 (2006).
- [17] J. Schroers, Adv. Mater. **22**, 1566 (2010).
- [18] A. Inoue, A. Takeuchi, Acta Mater. **59**, 2243 (2011).

- [19] C. Liu, E. Pineda, D. Crespo, *Metals* **5**, 1073 (2015).
- [20] M. A. Zeeshan, D. Esqué-de los Ojos, P. Castro-Hartmann, M. Guerrero, J. Nogués, S. Suriñach, M. D. Baró, B. J. Nelson, S. Pané, E. Pellicer et al., *Nanoscale*, 2016.
- [21] C.C. Hays, C. P. Kim, W. L. Johnson, *Physical Review Letters***84**(13), 2901 (2000).
- [22] C. Fan, R. T. Ott, T. C. Hufnagel, *Applied Physics Letters***81**(6), 1020 (2002).
- [23] D. C. Hofmann, J. Y. Suh, A. Wiest et al., *Nature***451**(7182), 1085 (2008).
- [24] D. C. Hofmann, J. Y. Suh, A. Wiest, W. Johnson, *ScriptaMaterialia***59**(7), 684 (2008).
- [25] Y. Wu, Y. Xiao, G. Chen, C. T. Liu, Z. Lu, *Advanced Materials***22**(25), 2770 (2010).
- [26] W. Diyatmika, J. P. Chu, B. T. Kacha, C.-C. Yu, C.-M. Lee, *Curr. Opin. Solid State Mater. Sci.* **19**, 95 (2015).
- [27] V. Chithambaram, S.J .Das, R.A. Nambi, K .Srinivasan, S. Krishnan *Physica B: Condensed Matter* 405 (12), 2605-2609